DOI: 10.1002/cmdc.200900017

Molecular Modeling and Molecular Dynamics Studies of Hydralazine with Human DNA Methyltransferase 1

Narender Singh,[a] Alfonso Dueñas-González,[b] Frank Lyko,[c] and Jose L. Medina-Franco*[a, d]

DNA methyltransferases (DNMTs) are a family of enzymes that methylate DNA at the C5 position of cytosine residues, and their inhibition is a promising strategy for the treatment of various developmental and proliferative diseases, particularly cancers. In the present study, a binding model for hydralazine, with a validated homology model of human DNMT, was developed by the use of automated molecular docking and molecular dynamics simulations. The docking protocol was validated by predicting the binding mode of 2′-deoxycytidine, 5-azacytidine, and 5-aza-2′-deoxycytidine. The inhibitory activity of hydralazine toward DNMT may be rationalized at the molecular level by similar interactions within the binding pocket (e.g., by a similar pharmacophore) as established by substrate-like deoxycytidine analogues. These interactions involve a complex network of hydrogen bonds with arginine and glutamic acid residues that also play a major role in the mechanism of DNA methylation. Despite the different scaffolds of other non-nucleoside DNMT inhibitors such as procaine and procainamide, the current modeling work reveals that these drugs exhibit similar interactions within the DNMT1 binding site. These findings are valuable in guiding the rational design and virtual screening of novel DNMT inhibitors.

1. Introduction

DNA methylation is an epigenetic change that results in the addition of a methyl group at the C5 position of cytosine residues. The process is mediated by DNA methyltransferases (DNMTs). To date, three DNMTs have been identified, including de novo DNMT3a and DNMT3b, and the maintenance DNMT1, which is the most abundant among the three.[1] DNMT1 is responsible for duplicating the pattern of DNA methylation during replication and is essential for mammalian development. These enzymes are key regulators of gene transcription, and their roles in carcinogenesis have been a topic of considerable interest in the last few years.[2] Diverse classes of compounds including nucleoside analogues, adenosine analogues, aminobenzoic derivatives, polyphenols, hydrazines, phthalides, disulfides, and antisense oligonucleotides are being discovered and evaluated as DNMT inhibitors. Currently, 5-azacytidine and 5-aza-2′-deoxycytidine (decitabine) are the only two that are approved by the US Food and Drug Administration (FDA) for the treatment of myelodysplastic syndrome.[3] However, whether their clinical efficacy in this condition results from their demethylating activities or by their intrinsic cytotoxicity remains to be fully elucidated.[4–7] Thus, specific inhibition of DNMT1 is an attractive and novel approach for cancer therapy.[8–12]

The various steps involved in the catalytic process of DNA cytosine C5 methylation are presented in Figure 1. DNA methylation is initiated by nucleophilic attack from a thiol group of a catalytic cysteine residue (Cys88) on the C6 position of the target cytosine, producing a covalent intermediate between the enzyme and the base (Figure 1). (Residue numbers used throughout this study are based on the sequence alignment shown in figure S1 of the Supporting Information.) Following this, the C5 position of cytosine is activated and performs a nucleophilic attack on the methyl group of the methyl-donating cofactor *S*-adenosyl-L-methionine (AdoMet). The attack on the C6 atom is facilitated by transient protonation of the cytosine ring at the endocyclic nitrogen atom N3, stabilized by a glutamate residue (Glu128). The high-energy carbanion may also be stabilized by resonance,[13] in which an arginine residue (Arg174) plays an important role in the catalytic mechanism.[14] The covalent complex between the methylated base and the DNA is resolved by deprotonation at the C5 position, which leads to re-establishment of aromaticity. The methylated base is then released along with *S*-adenosyl-L-homocysteine (AdoHyc).

The inhibitors 5-azacytidine and decitabine (Figure 2) cause substantial cytotoxicity. The former becomes incorporated into RNA, whereas decitabine incorporates into DNA.[16] These compounds cause significant myelotoxicity and also have low sta-

[a] *Dr. N. Singh, Dr. J. L. Medina-Franco*
Torrey Pines Institute for Molecular Studies
11350 SW Village Parkway, Port St. Lucie, FL 34987 (USA)
Fax: (+1) 772-345-4685
E-mail: jmedina@tpims.org

[b] *Dr. A. Dueñas-González*
Unidad de Investigación Biomédica en Cáncer
Instituto de Investigaciones Biomédicas
Universidad Nacional Autónoma de México
Instituto Nacional de Cancerología, Mexico City (Mexico)

[c] *Dr. F. Lyko*
Division of Epigenetics, Deutsches Krebsforschungszentrum
Im Neuenheimer Feld 580, 69120 Heidelberg (Germany)

[d] *Dr. J. L. Medina-Franco*
Division of Basic Research, Instituto Nacional de Cancerología
Av. San Fernando 22, Mexico City 14080 (Mexico)

Supporting information for this article is available on the WWW under http://dx.doi.org/10.1002/cmdc.200900017.

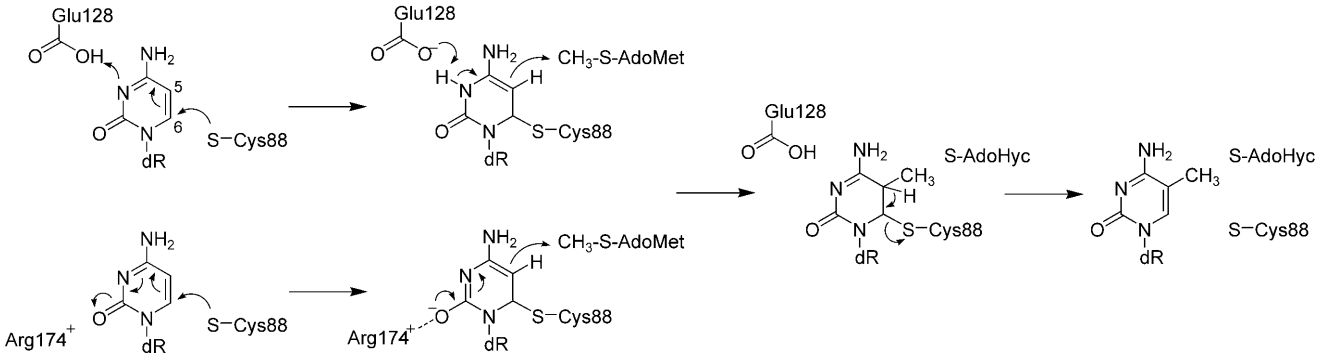

Figure 1. Reaction mechanism of DNA cytosine C5 methylation: adapted from Kumar et al.[13] and Hermann et al.[15] Amino acid residue numbers are based on the homology model. Equivalent residue numbers in the M.Hal crystal structure of residues shown here are Cys81, Glu119, and Arg165.

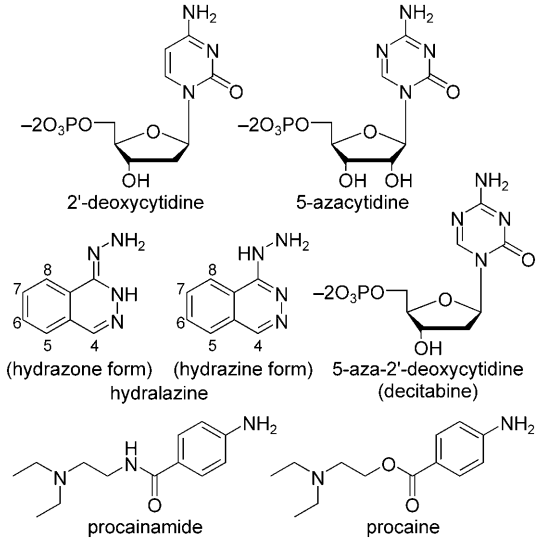

Figure 2. Structures of DNA methyltransferase inhibitors studied in this work. Two tautomeric forms of hydralazine are depicted.

bility.[17] Because nucleoside inhibitors are cytotoxic on their own,[18] much emphasis has been put on the development of compounds that target DNA methyltransferases without being incorporated into RNA or DNA. Alternative DNMT inhibitors include the known drugs procainamide, procaine, and hydralazine, which are commonly used as antiarrhythmic, local anesthetic, and antihypertensive drugs, respectively (Figure 2).[19] Additional DNMT inhibitors are the polyphenol compound from green tea extract, (−)-epigallocatechin-3-gallate (EGCG)[20] and RG108, which was discovered by a docking-based virtual screening methodology based on a homology model of human DNMT1.[21] A binding model of EGCG within the catalytic domain of DNMT1 has also been proposed.[20]

The cardiovascular drugs hydralazine and procainamide have shown demethylation and tumor suppression-reactivation activity.[22–24] Furthermore, it has been suggested that procaine and procainamide are DNMT1 inhibitors that bind to the DNA and hence cause demethylation and growth-inhibitory effects in cancer cells.[25,26] Hydralazine is currently under evaluation in clinical trials for cancer, mainly in combination with a histone deacetylase inhibitor.[27] To gain insight into the binding mode and interactions of hydralazine and other inhibitors described above with DNMT1, and to consequently improve the development of novel inhibitors, we describe herein a study of the docking and molecular dynamics (MD) simulations of hydralazine with DNMT1. Although a binding model of hydralazine with DNMT1 was proposed in a previous study,[28] it was neither compared with the binding mode of 5-azacytidine and its analogues and other non-nucleoside inhibitors, nor did it provide a mechanistic interpretation of the inhibitory activity of hydralazine. In this work, we extend our previous docking studies by modeling the two possible tautomeric forms of hydralazine with a previously validated homology model of DNMT1.[29] The docking models developed in this work were further studied and refined with 3 ns MD simulations. The models thus generated suggest putative pharmacophoric groups of hydralazine and modifications that may optimize its activity. Comparison of the binding model of hydralazine with those of 5-azacytidine and its analogues, as well as procainamide and procaine, reveal common interactions within the DNMT1 binding site. These findings will be valuable for the further optimization, design, and virtual screening of novel DNMT1 inhibitors.

2. Methods

2.1. Docking

Molecular Operating Environment (MOE) 2007[30] was used for ligand and protein preparation and molecular structure viewing. All the docking calculations were conducted with AutoDock 3.0.[31] In short, AutoDock performs an automated docking of the ligand with user-specified dihedral flexibility within a rigid binding site of the receptor. The program performs several runs in each docking experiment. Each run provides one predicted binding mode.

A previously established homology model of human DNMT1 was used. Briefly, this model was built through sequence alignment of human DNMT1 based on multiple structures of aligned M.HhaI (6MHT), M.HaeIII (1DCT), and DNMT2 (1G55) protein sequences.[29] Polar hydrogen atoms were added, and

Kollman charges,[32] atomic salvation parameters, and fragmental volumes were assigned to the protein using AutoDockTools. Notably, after assigning protonation states with AutoDockTools, the side chains of basic residues were protonated, and the side chains of acidic residues were not protonated. For hydralazine, procainamide, and procaine, Gasteiger charges[33] were assigned, and nonpolar hydrogen atoms were merged. All torsions were allowed to rotate during docking.

The auxiliary program AutoGrid generated the grid maps. First, to dock 2′-deoxycytidine, each grid was centered at Cα of the catalytic cysteine (Cys88). Then, each grid was centered at the center of coordinates of docked 2′-deoxycytidine. The grid dimensions were 60×40×40 points separated by a grid spacing of 0.375 Å. Lennard–Jones parameters 12-10 and 12-6, supplied with the program, were used for modeling hydrogen bonds and van der Waals (vdW) interactions, respectively. The distance-dependent dielectric permittivity of Mehler and Solmajer[34] was used for calculation of the electrostatic grid maps. For hydralazine, procainamide, and procaine, random starting positions, random orientations, and torsions were used. The translation, quaternion, and torsions steps were taken from default values in AutoDock. The Lamarckian genetic algorithm and the pseudo-Solis and Wets methods were applied for minimization using default parameters. The number of docking runs was 100. The population in the genetic algorithm was 150, the energy evaluations were 250000, and the maximum number of iterations was 27000. After docking, the 100 solutions were clustered into groups with RMSDs <1.5 Å.

To describe the ligand binding pocket interactions, the top-ranked binding mode found by AutoDock in complex with the binding pocket of DNMT was subject to full energy minimization using the MMFF94x force field implemented in MOE until a gradient of 0.05 was reached. The default parameters implemented into the LigX application of MOE were used.[30]

2.2. Molecular dynamics

MD simulations were performed for the binding models of the two tautomeric forms of hydralazine and 2′-deoxycytidine using the NAMD2 program[35] with the CHARMM 29b2 force field.[36] The initial docked and refined structures from previous steps were taken as starting points for MD simulation. The system setup procedure was initiated by adding hydrogen atoms and a box of TIP3 water molecules (solvation), such that there was at least 13.0 Å of water between the surface of the protein and the edge of the simulation box, using the Solvate plug-in of the Visual Molecular Dynamics (VMD) program.[37] Any added bulk water molecules within 2.5 Å of the protein were excluded. To maintain charge neutrality of the system, appropriate numbers of ions were added using the Autoionize plug-in in VMD; these were initially at least 7.0 Å away from the surface of the protein. The final resulting systems contained 58284, 58239, and 58507 atoms for hydrazine-, hydrazone-, and 2′-deoxycytidine-bound systems, respectively.

3. Results and Discussion

The three-dimensional (3D) structures of DNA methyltransferase are currently available only for the bacterial methylases and the putative human DNA methyltransferase, DNMT2. In this work, we used a homology model for human DNMT1 based on the template structures of the available M.HhaI (6MHT),[13] M.HaeIII (1DCT),[38] and DNMT2 (1G55)[39] protein crystal structures.[29] This model was recently used in the successful discovery of a novel DNMT inhibitor (RG108) through docking-based virtual screening.[21]

3.1. Validation of the docking protocol

The docking protocol was validated by predicting and comparing the binding mode of substrate 2′-deoxycytidine and its analogues 5-azacytidine and 5-aza-2′-deoxycytidine. The calculated binding energies with AutoDock are summarized in Table 1.

Table 1. Docking results of DNMT1 inhibitors.

Compound	E_{docked} [kcal mol^{-1}]	ΔG [kcal mol^{-1}]
2′-deoxycytidine	−15.8	−14.4
5-azacytidine	−16.2	−14.7
5-aza-2′-deoxycytidine	−15.7	−14.3
hydralazine (hydrazone tautomer)	−7.4	−7.4
hydralazine (hydrazine tautomer)	−7.7	−7.3
procainamide	−10.5	−8.1
procaine	−10.3	−8.0

Figures 3A and 3B respectively show 2D optimized docked models of 2′-deoxycytidine and 5-aza-2′-deoxycytidine with DNMT1. Residues that are common to the binding pockets of the deoxycytidine analogues are Pro86, Cys88, Glu128, Arg172, Arg174, Thr320, His321, Gly440, and Asn441. In all cases, several hydrogen bonds are predicted between the side chain of Arg174 and a number of oxygen atoms, including those at the cytosine and pentose rings and the phosphate group. Notably, the interaction with the carbonyl oxygen of the cytosine ring seems to play a key role in the mechanism of methylation through stabilization of the intermediate formed after the nucleophilic attack of AdoMet (Figure 1). Similar interactions are observed in the crystal structure of bacterial M.HhaI between the corresponding arginine (Arg165 in the M.HaI crystal structure 6MHT) and the co-crystallized 4′-thio-2′-deoxycydidine.[13] A second hydrogen bond is predicted between the side chain of Glu128 and the amino group of the cytosine ring. Notably, Glu128 is close to N3 of cytosine and also seems to participate in the methylation mechanism by stabilization of the intermediate. Similar interactions are observed in the crystal structure of the bacterial M.HhaI (Glu119 in the M.HaI crystal structure 6MHT). A third hydrogen bond is also predicted between the backbone nitrogen atom of His321 with the 3′-hydroxy group of cytidine. His321 in DNMT1 is substituted with alanine at the corresponding position in M.HhaI and M.HaeIII (Ala253 in M.HaI crystal structure 6MHT). Similar interactions were ob-

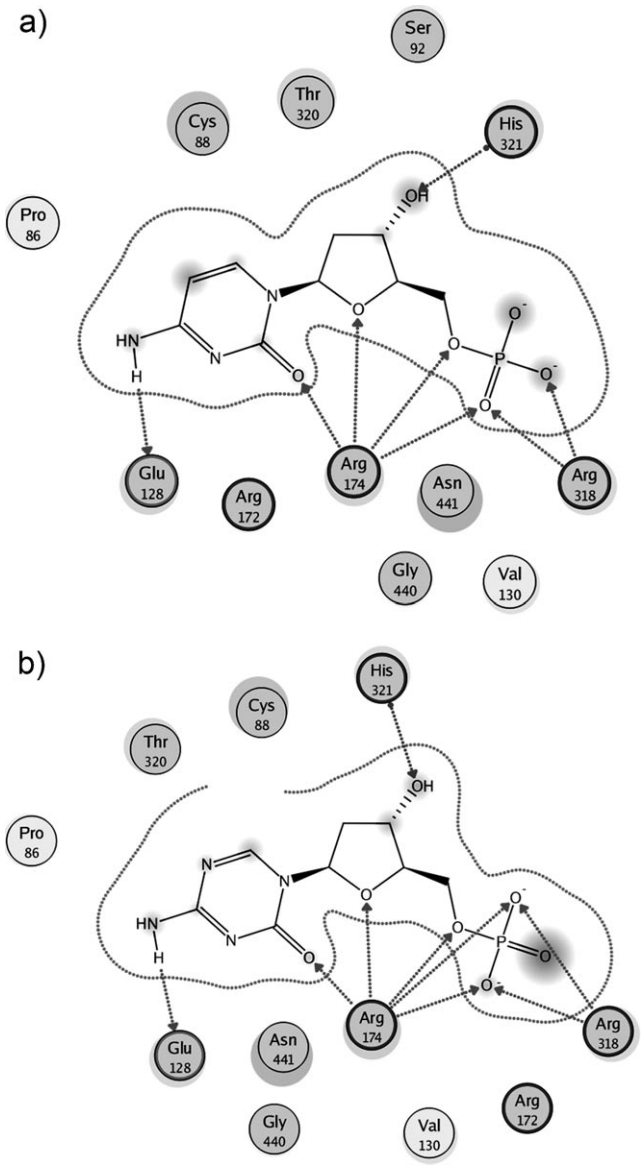

Figure 3. Optimized docking models of a) 2′-deoxycytidine and b) 5-aza-2′-deoxycytidine with the homology model of human DNMT1. Arrows indicate hydrogen bonding. "Clouds" on ligand atoms indicate the solvent-exposed surface area of ligand atoms (darker and larger clouds mean more solvent exposure). "Halos" around residues indicate the degree of interaction with ligand atoms (larger, darker halos mean greater interaction). The dotted contour reflects steric room for methyl substitution. The contour line is broken if it is closest to an atom which is fully exposed.

served in the optimized docking model of 5-azacytidine (figure S2, Supporting Information). These observations suggest that AutoDock successfully predicted the binding modes of the deoxycytidine analogues.

The 3 ns MD simulations of the optimized docking model of 2′-deoxycytidine also revealed the stability of the model, as evident in the RMSD plot of the (backbone atoms of the secondary structures) obtained trajectory (Figure 4). The simulations of 2′-deoxycytidine further revealed the importance (stability) and complexity of the hydrogen bonds between Glu128 and the amino group of cytosine, and the Arg174 side chain

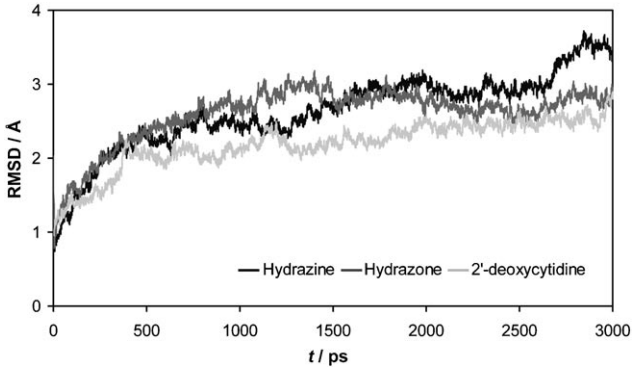

Figure 4. RMSD plot of the backbone atoms of the secondary structures during MD simulation of hydrazone, hydrazine, and 2′-deoxycytidine within the DNMT1 binding site. The plot reflects the stability of the systems during the simulations.

with the carbonyl oxygen of the cytosine ring. MD simulations also point to a partially stable hydrogen bond with Ser92 and Gly93.

3.2. Docking of hydralazine, procainamide, and procaine

Hydralazine may be present in two tautomeric forms, the imino form (hydrazone tautomer) and the amino form (hydrazine tautomer) (Figure 2). A key structural difference between the two tautomers is the position of the hydrogen atom at the N2 nitrogen of the phthalazine ring. In a previous docking study of hydralazine with DNMT1, only the hydrazine form was considered.[28] In the present work, we docked both tautomeric forms within the catalytic site of DNMT1 in order to define a more precise role for the four nitrogen atoms in binding, and to identify potential sites of substitution to enhance the activity of hydralazine. The details of the docking results are summarized in Table 1. Both tautomers showed a very similar docking and interaction energy with DNMT1. Thus, based on the energies calculated with docking, both tautomers may have the same probability of binding with the enzyme. The calculated interaction energy with AutoDock is higher than the docking energy calculated for 5-azacytidine and its analogues.

Figures 5 A and 5 B depict the 2D interaction maps of the optimized binding modes of hydrazone and hydrazine with DNMT1, respectively. Both binding models are similar in the general orientation of the hydralazine core in the binding pocket. In their similarity, both tautomers form hydrogen bonds with the side chains of Glu128 and Arg174. In both tautomeric forms, three or four nitrogen atoms of hydralazine appear to play an important role in the interaction with DNMT1. According to the docking models, a notable difference between the binding modes of the two tautomeric forms is that the hydrazone tautomer makes a bidentate hydrogen bond with Glu128. This interaction cannot happen for the amino tautomer. However, the amino tautomer is capable of forming a more extensive network of hydrogen bonds with Arg172 and Ala442 as well, as determined by MD simulation studies (see below).

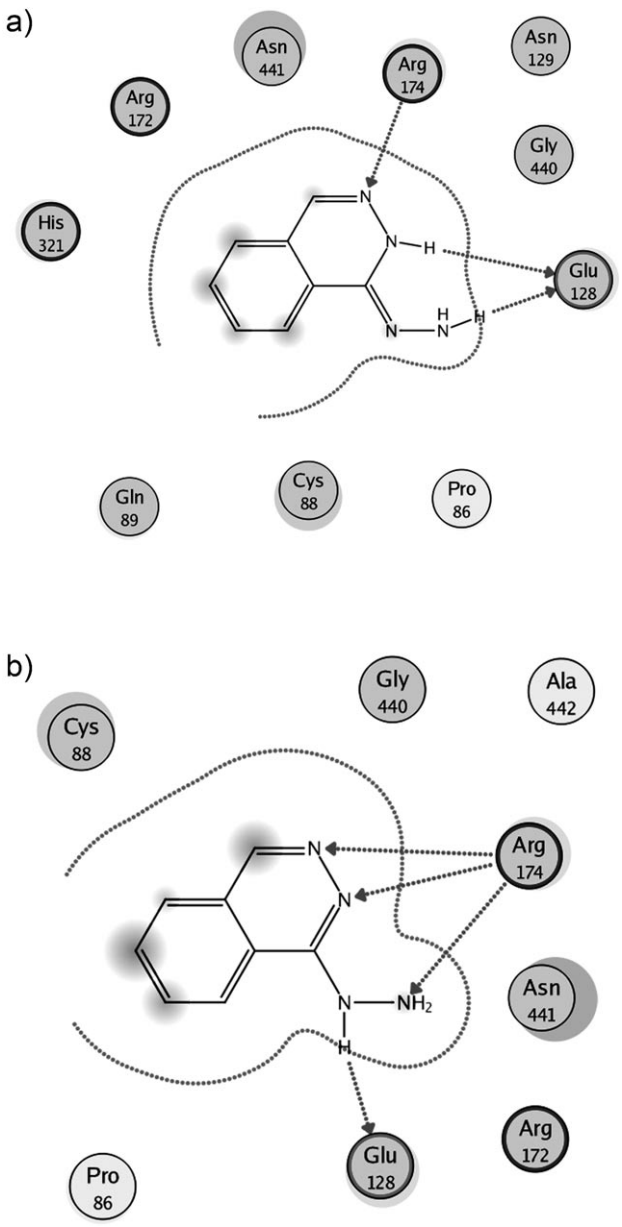

Figure 5. Optimized binding models for hydralazine in a) the hydrazone tautomer (imino form) and b) the hydrazine tautomer (amino form). The image features are the same as those described for Figure 3.

Figures 6A and 6B show a comparison of the binding modes of the tautomeric forms of hydralazine with 2′-deoxycytidine. Notably, three nitrogen atoms of hydralazine in the hydrazone tautomer roughly overlap with three heteroatoms of 2′-deoxycytidine (Figure 6A). The amino group of the hydrazone tautomer occupies the same binding position as the amino group of cytosine and is capable of forming a hydrogen bond with Glu128. The protonated nitrogen of the phthalazine ring also roughly occupies the same binding position as that of N3 and resembles the transient protonation state of the cytosine ring at the nitrogen atom N3 that is stabilized by the glutamate residue during the methylation of cytosine. Finally, the unprotonated nitrogen atom of the phthalazine ring in the hydrazone form also roughly overlaps with the binding position of the carbonyl oxygen of cytosine. Either nitrogen atom in hydralazine and oxygen in cytosine are acceptors in the hydrogen bond with Arg174.

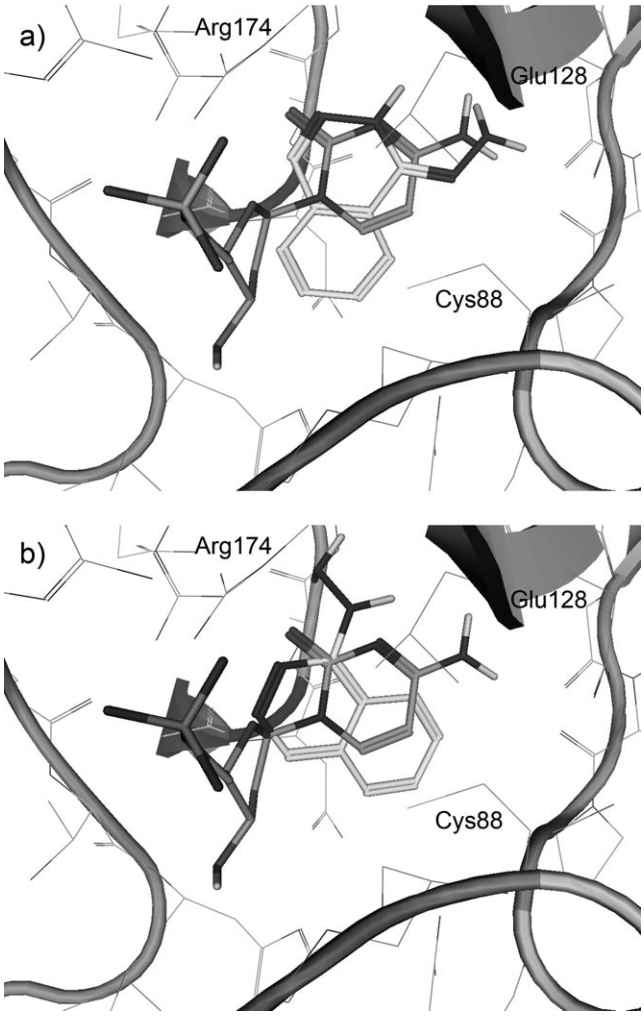

Figure 6. Comparison of the optimized binding models of hydralazine with the binding model of 2′-deoxycytidine (carbon atoms in dark gray): a) hydrazone tautomer, b) hydrazine tautomer: carbon atoms in light gray. Nonpolar hydrogen atoms are omitted for clarity.

Docking models for the two tautomeric forms of hydralazine were also compared with the docking of the deoxycytidine analogues procaine and procainamide. For both compounds, there is experimental evidence of their interaction with DNMT1,[26] but no docking models have been reported. The docking results for these compounds are also summarized in Table 1. The calculated free energy of binding (ΔG) calculated with AutoDock for hydralazine is higher than the interaction energy calculated for any of the other DNMT1 inhibitors (Table 1). This may be expected, at least in part, from the smaller size of the hydralazine molecule (the calculated solvent-accessible surface area of procaine and procainamide is ~490 Å^2, whereas for hydrazine and hydrazone, it is ~310 and 346 Å^2, respectively).

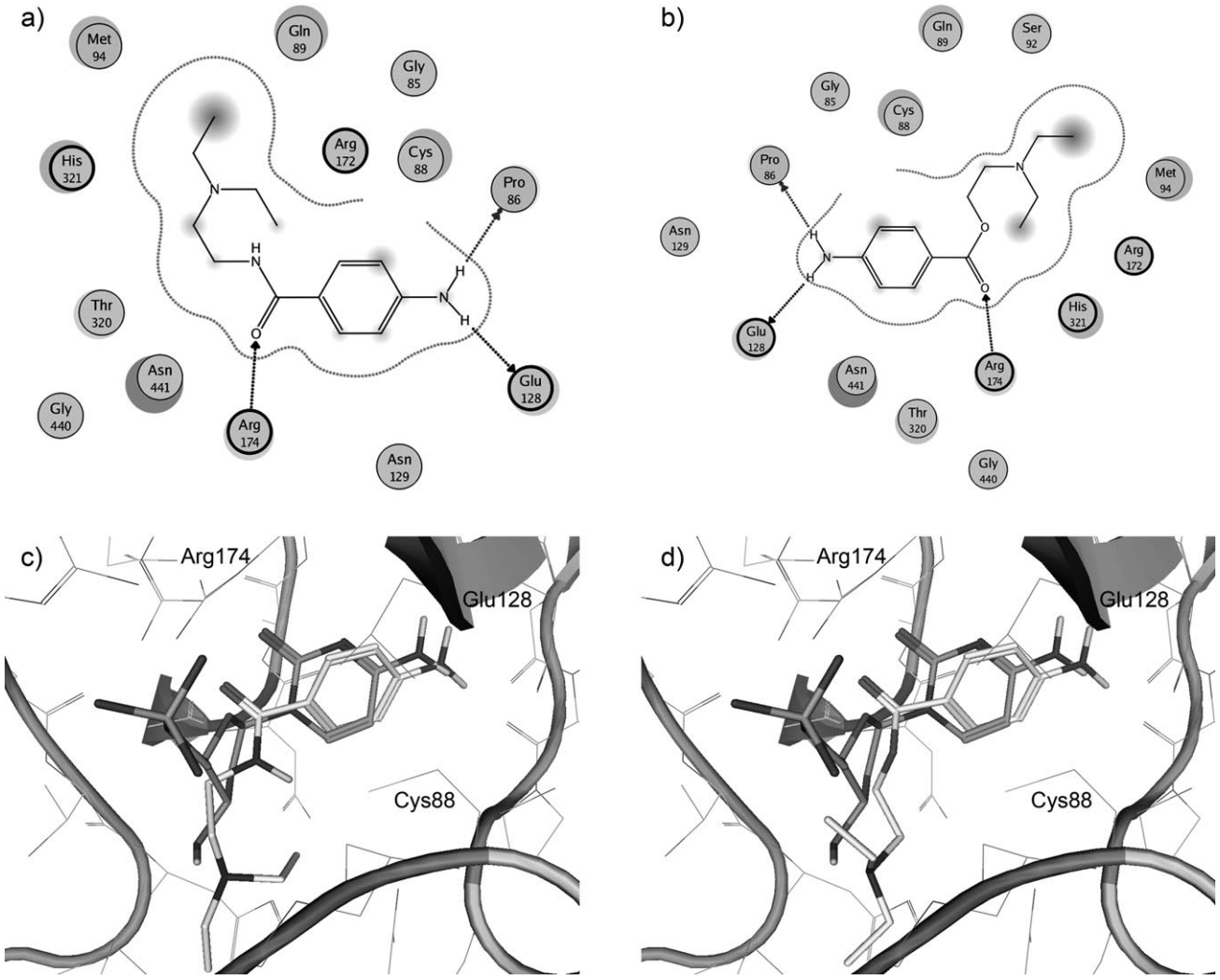

Figure 7. 2D interaction diagram for the optimized docking models of a) procainamide and b) procaine. Comparison of the binding mode of 2′-deoxycitidine (carbon atoms in dark gray) with c) procainamide and d) procaine (carbon atoms in light gray). Nonpolar hydrogen atoms are omitted for clarity. Note the similar positions of the amino groups and the very similar position of the carbonyl oxygen of procainamide and procaine with the ribose oxygen. These atoms form hydrogen bonds with Glu128 and Arg174, respectively. The image features are same as those described for Figure 3.

The two nitrogen atoms of the phthalazine ring of the hydrazine tautomer occupy a similar binding position as the carbonyl oxygen and the 4′-oxygen atom of the ribose ring (Figure 6B). These two atoms, either nitrogen in the hydrazine tautomer or oxygen in cytidine, act as hydrogen bond acceptors in interacting with Arg174. The secondary amine group of the hydrazine tautomer is also close to the binding position of N3 of cytidine, and may resemble the protonated state of N3 that seems to be formed during the methylation of cytosine. In fact, a hydrogen bond is predicted between the secondary amine group of the hydrazine tautomer with Glu128.

Interestingly, the binding models of procainamide and procaine developed in this work also show the capacity of these molecules to form hydrogen bonds with Glu128 and Arg174. Overall, the predicted binding modes of these two drugs are very similar to those of 2′-deoxycytidine and other deoxycytidine analogues. Figure 7 shows the very similar positioning of the amino groups of procaine and procainamide in the binding site. Moreover, the carbonyl oxygen of procainamide and procaine occupy roughly the same position as that of the oxygen of the ribose ring of 2′-deoxycytidine in making hydrogen bonds with Arg174.

3.3. MD simulations of hydralazine and 2′-deoxycytidine

To further investigate the structural stability, dynamics, and key ligand–receptor interaction patterns of binding models generated with docking for the tautomeric form of hydralazine, an MD simulation for 3 ns in explicit solvent was performed. For comparison, the simulation of 2′-deoxycytidine was also carried out.

From the RMSD of protein (Figure 4), it is clear that all the complexes are very stable throughout the simulation, with 2′-deoxycytidine, not surprisingly, being the most stable.

Hydrogen bond probability calculated from analyzing the simulations shows that for the hydrazine form, Glu128 forms a

bidentate hydrogen bond with the hydrazine moiety, and Arg174 makes several hydrogen bonds (H-bond donor) with the hydrazine moiety and the phthalazine ring. For the hydrazone tautomer, several (stable) hydrogen bonds with Arg174 were also predicted.

In MD simulations of both tautomeric forms of hydralazine, the terminal amino group shows the major degree of vdW contacts with the binding pocket of DNMT1. In order to gain insight into the structural stability of the tautomeric forms of hydralazine, the vdW and electrostatic components of both the forms were calculated and are shown in Figure 8.

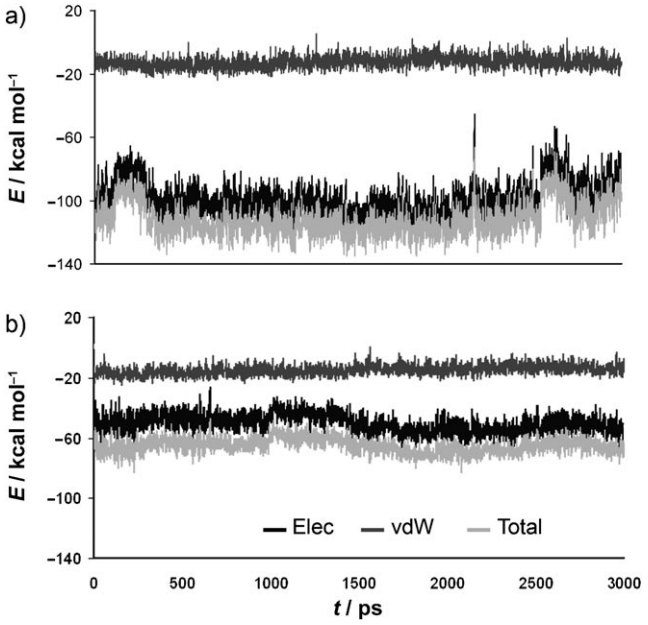

Figure 8. The electrostatic, van der Waals, and total interaction energy plot versus simulation time of 3 ns is shown for a) hydrazine and b) hydrazone.

As expected, the amino form (avg. -112 kcal mol^{-1}) was much more stable than the imino form (avg. -65 kcal mol^{-1}) due to its flexible side chain, which is conformationally more available to make hydrogen bond and electrostatic interactions with the binding site residues (other components of the total energy, i.e., bond, angle, dihedral, and vdW, are very similar for both the tautomers). Hence, these calculations suggest that, in solution, if both tautomers are present, then hydrazine–DNMT1 binding will be more stable than the hydrazone–DNMT1 complex.

From MD simulations, the flexibility of the binding site was also predicted. The calculated RMS fluctuations of the residues showed that residues Met94, Ser92, Gln89, Cys88, and Arg172 are highly flexible (fluctuations between 1.5 and 3 Å). Among these, residues Met94, Ser92, and Gln89 lie at the entrance of the binding site, whereas residues Cys88 and Arg172 are part of core binding site. In virtual screening studies of DNMT1 inhibitors, special emphasis should be given to these residues, which may aid in better selection of inhibitors.

3.4. Strategies to optimize hydralazine

Based on our docking and MD simulation studies, we propose the C5 position of hydralazine (Figure 2) as an attractive position to introduce additional substituents to enhance the affinity with DNMT1. Our results show that there is space to include a bulky group at this position that may improve the fit of these compounds in the binding site. In MD simulations, the hydrogen atom at C5 has an average of only seven vdW contacts with DNMT1 (vdW contacts were calculated based on protein atoms within 4.2 Å of the query). Another attractive position to enhance the activity of hydralazine is C4 (Figure 2). MD simulations reveal average vdW contacts with DNMT1 of 6.8 Å for the hydrazine tautomer and 8.19 Å for the hydrazone tautomer at this position. Both C5 and C4 atoms of the hydralazine sit in a pocket that is open to the outside and is surrounded by polar residues Asn440, Gln89, Pro87, and His321 on top and bottom. Comparison of the optimized docking models of hydralazine (both tautomers) with 2′-deoxycytidine also shows that the C4 position of hydralazine is oriented in roughly the same position as the ribose ring of 2′-deoxycytidine. Thus, the introduction of a bulky group, such as an aromatic ring, at C4 of hydralazine may enhance the affinity with DNMT1.

4. Conclusions

The ability of hydralazine to induce DNA demethylation has been a matter of controversy.[19,40,41] This suggests that hydralazine is a comparably weak inhibitor of DNA methyltransferases that can show increased inhibitory potency under certain experimental conditions. Consistent with this notion, the predicted free energy of binding for hydralazine appeared less favorable than that of nucleoside analogues and other non-nucleoside demethylating drugs. At the same time, this also suggests that the hydralazine scaffold can be optimized to increase the affinity of hydralazine derivatives for DNMT1 and other DNA methyltransferases.

In this work, we docked hydralazine, procaine, and procainamide with a homology model of DNMT1. The docking protocol was validated by predicting the binding modes of 2′-deoxycytidine, 5-azacytidine, and 5-aza-2′-deoxycytidine. Docked models were further refined, and dynamics of selected systems were investigated through molecular dynamics studies. Our results suggest that among the two tautomeric forms of hydralazine, the hydrazine–DNMT1 complex is more stable than the hydrazone–DNMT1 complex. These results also highlight the interaction of these compounds with the arginine and glutamic acid residues that play a major role in the mechanism of DNA methylation. These observations may direct future studies of novel DNMT1 inhibitors. In this regard, virtual screening of compound databases will be carried out to search for better and novel inhibitors, and our results will be communicated in a forthcoming paper.

Supporting Information

The Supporting Information contains the amino acid sequence numbers used in this study along with a 2D interaction diagram for the optimized docking model of 5-azacytidine (figure S1 and S2, respectively).

Acknowledgements

This work was supported by the State of Florida, Executive Office of the Governor's Office of Tourism, Trade, and Economic Development. Dr. Dueñas-González's work has been supported by the Catedra Instituto Científico Pfizer-PUIS, UNAM. The authors are also grateful to A. Olson and colleagues for providing AutoDock.

Keywords: DNA methylation · docking · drug design · epigenetics · molecular dynamics

[1] H. Lei, S. P. Oh, M. Okano, R. Juttermann, K. A. Goss, R. Jaenisch, E. Li, *Development* **1996**, *122*, 3195–3205.
[2] Y. Kanai, *Pathol. Int.* **2008**, *58*, 544–558.
[3] N. Yu, M. Wang, *Curr. Med. Chem.* **2008**, *15*, 1350–1375.
[4] K. Schmelz, N. Sattler, M. Wagner, M. Lubbert, B. Dorken, I. Tamm, *Leukemia* **2005**, *19*, 103–111.
[5] S. M. Pulukuri, J. S. Rao, *Int. J. Oncol.* **2005**, *26*, 863–871.
[6] G. Chai, L. Li, W. Zhou, L. Wu, Y. Zhao, D. Wang, S. Lu, Y. Yu, H. Wang, M. A. McNutt, Y. G. Hu, Y. Chen, Y. Yang, X. Wu, G. A. Otterson, W. G. Zhu, *PLoS One* **2008**, *3*, e2445.
[7] S. S. Palii, B. O. Van Emburgh, U. T. Sankpal, K. D. Brown, K. D. Robertson, *Mol. Cell. Biol.* **2008**, *28*, 752–771.
[8] M. Szyf, *Trends Pharmacol. Sci.* **1994**, *15*, 233–238.
[9] M. Szyf, *Cancer Metastasis Rev.* **1998**, *17*, 219–231.
[10] G. Strathdee, R. Brown, *Expert Opin. Invest. Drugs* **2002**, *11*, 747–754.
[11] B. Brueckner, D. Kuck, F. Lyko, *Cancer J.* **2007**, *13*, 17–22.
[12] F. Lyko, R. Brown, *J. Natl. Cancer Inst.* **2005**, *97*, 1498–1506.
[13] S. Kumar, J. R. Horton, G. D. Jones, R. T. Walker, R. J. Roberts, X. Cheng, *Nucleic Acids Res.* **1997**, *25*, 2773–2783.
[14] T. P. Jurkowski, M. Meusburger, S. Phalke, M. Helm, W. Nellen, G. Reuter, A. Jeltsch, *RNA* **2008**, *14*, 1663–1670.
[15] A. Hermann, H. Gowher, A. Jeltsch, *Cell. Mol. Life Sci.* **2004**, *61*, 2571–2581.
[16] A. Cihak, *Oncology* **1974**, *30*, 405–422.
[17] J. C. Cheng, C. B. Matsen, F. A. Gonzales, W. Ye, S. Greer, V. E. Marquez, P. A. Jones, E. U. Selker, *J. Natl. Cancer Inst.* **2003**, *95*, 399–409.
[18] R. Juttermann, E. Li, R. Jaenisch, *Proc. Natl. Acad. Sci. USA* **1994**, *91*, 11797–11801.
[19] C. Arce, B. Segura-Pacheco, E. Perez-Cardenas, L. Taja-Chayeb, M. Candelaria, A. Dueñas-González, *J. Transl. Med.* **2006**, *4*, 10.
[20] M. Z. Fang, Y. Wang, N. Ai, Z. Hou, Y. Sun, H. Lu, W. Welsh, C. S. Yang, *Cancer Res.* **2003**, *63*, 7563–7570.
[21] P. Siedlecki, R. G. Boy, T. Musch, B. Brueckner, S. Suhai, F. Lyko, P. Zielenkiewicz, *J. Med. Chem.* **2006**, *49*, 678–683.
[22] B. Segura-Pacheco, C. Trejo-Becerril, E. Perez-Cardenas, L. Taja-Chayeb, I. Mariscal, A. Chavez, C. Acuña, A. M. Salazar, M. Lizano, A. Dueñas-González, *Clin. Cancer Res.* **2003**, *9*, 1596–1603.
[23] Y. Song, C. Zhang, *Cancer Chemother. Pharmacol.* **2009**, *63*, 605–613.
[24] A. Y. Law, K. P. Lai, C. K. Ip, A. S. Wong, G. F. Wagner, C. K. Wong, *Exp. Cell Res.* **2008**, *314*, 1823–1830.
[25] B. H. Lee, S. Yegnasubramanian, X. Lin, W. G. Nelson, *J. Biol. Chem.* **2005**, *280*, 40749–40756.
[26] A. Villar-Garea, M. F. Fraga, J. Espada, M. Esteller, *Cancer Res.* **2003**, *63*, 4984–4989.
[27] A. Dueñas-González, M. Candelaria, C. Perez-Plascencia, E. Perez-Cardenas, E. de La Cruz-Hernandez, L. A. Herrera, *Cancer Treat. Rev.* **2008**, *34*, 206–222.
[28] E. Angeles, V. H. Vazquez-Valadez, O. Vazquez-Valadez, A. M. Velazquez-Sanchez, A. Ramirez, L. Martinez, S. Diaz-Barriga, A. Romero-Rojas, G. Cabrera, R. Lopez-Castanares, A. Dueñas-González, *Lett. Drug Des. Discovery* **2005**, *2*, 282–286.
[29] P. Siedlecki, R. G. Boy, S. Comagic, R. Schirrmacher, M. Wiessler, P. Zielenkiewicz, S. Suhai, F. Lyko, *Biochem. Biophys. Res. Commun.* **2003**, *306*, 558–563.
[30] *Molecular Operating Environment (MOE)*, version **2007,** Chemical Computing Group Inc., Montreal, QC (Canada): http://www.chemcomp.com (accessed January 14, 2009).
[31] G. M. Morris, D. S. Goodsell, R. S. Halliday, R. Huey, W. E. Hart, R. K. Belew, A. J. Olson, *J. Comput. Chem.* **1998**, *19*, 1639–1662.
[32] S. J. Weiner, P. A. Kollman, D. A. Case, U. C. Singh, C. Ghio, G. Alagona, S. Profeta, P. Weiner, *J. Am. Chem. Soc.* **1984**, *106*, 765–784.
[33] J. Gasteiger, M. Marsili, *Tetrahedron* **1980**, *36*, 3219–3228.
[34] E. L. Mehler, T. Solmajer, *Protein Eng.* **1991**, *4*, 903–910.
[35] J. C. Phillips, R. Braun, W. Wang, J. Gumbart, E. Tajkhorshid, E. Villa, C. Chipot, R. D. Skeel, L. Kale, K. Schulten, *J. Comput. Chem.* **2005**, *26*, 1781–1802.
[36] B. R. Brooks, R. E. Bruccoleri, B. D. Olafson, D. J. States, S. Swaminathan, M. Karplus, *J. Comput. Chem.* **1983**, *4*, 187–217.
[37] W. Humphrey, A. Dalke, K. Schulten, *J. Mol. Graph.* **1996**, *14*, 33–38.
[38] K. M. Reinisch, L. Chen, G. L. Verdine, W. N. Lipscomb, *Cell* **1995**, *82*, 143–153.
[39] A. Dong, J. A. Yoder, X. Zhang, L. Zhou, T. H. Bestor, X. Cheng, *Nucleic Acids Res.* **2001**, *29*, 439–448.
[40] A. Chavez-Blanco, C. Perez-Plasencia, E. Perez-Cardenas, C. Carrasco-Legleu, E. Rangel-Lopez, B. Segura-Pacheco, L. Taja-Chayeb, C. Trejo-Becerril, A. Gonzalez-Fierro, M. Candelaria, G. Cabrera, A. Dueñas-González, *Cancer Cell Int.* **2006**, *6*, 2.
[41] J. C. Chuang, C. B. Yoo, J. M. Kwan, T. W. Li, G. Liang, A. S. Yang, P. A. Jones, *Mol. Cancer Ther.* **2005**, *4*, 1515–1520.

Received: January 14, 2009
Revised: February 12, 2009
Published online on ■■ ■■, 2009

A series of DNA methyltransferase 1 (DNMT1) inhibitors were modeled by docking and molecular dynamics studies to rationalize their activity. Our findings will be valuable in guiding research efforts toward the rational design and virtual screening of novel DNMT inhibitors.

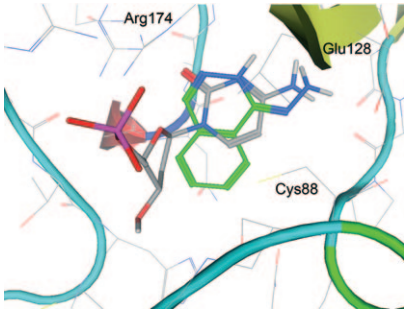

*N. Singh, A. Dueñas-González, F. Lyko, J. L. Medina-Franco**

■■ – ■■

Molecular Modeling and Molecular Dynamics Studies of Hydralazine with Human DNA Methyltransferase 1

